Whole genome CRISPR screens identify LRRK2-regulated endocytosis as a major mechanism for extracellular tau uptake by human neurons

Lewis D. Evans[1,2], Alessio Strano[1], Ashley Campbell[1,2], Emre Karakoc[2,3], Francesco Iorio[2,3], Andrew R. Bassett[2,3], and Frederick J. Livesey[1,2*]

[1]UCL Great Ormond Street Institute of Child Health, Department of Developmental Biology and Cancer, Zayed Centre for Research into Rare Disease in Children, 20 Guilford Street, London WC1N 1DZ, UK

[2]Open Targets, Wellcome Genome Campus, Cambridge CB10 1SA, UK.

[3] Wellcome Sanger Institute, Wellcome Genome Campus, Cambridge CB10 1SA, UK.

[*]Author for correspondence: r.livesey@ucl.ac.uk

ABSTRACT

Pathological protein aggregation in Alzheimer's disease and other dementias is proposed to spread through the nervous system by a process of intercellular transfer of pathogenic forms of tau protein. Defining the cellular mechanisms of tau entry to human neurons is essential for understanding dementia pathogenesis and the rational design of disease-modifying therapeutics. Using whole genome CRISPR knockout screens in human iPSC-derived excitatory neurons, the primary cell type affected in these diseases, we identified genes and pathways required specifically for uptake of monomeric and aggregated tau. Monomeric and aggregated tau are both taken up by human neurons by receptor-mediated endocytosis, with the low-density lipoprotein LRP1 a significant surface receptor for both forms of tau. Perturbations of the endolysosome and autophagy systems at many levels, and specifically endosome sorting and receptor recycling, greatly reduced tau uptake. Of particular therapeutic interest is that loss of function of the endocytosis and autophagy regulator LRRK2, as well as acute inhibition of its kinase activity, reduced neuronal uptake of monomeric and aggregated tau. Kinase-activating mutations in LRRK2 are a cause of Parkinson's disease accompanied by neuronal tau aggregation, suggesting that LRRK2 mediates tau spreading *in vivo* and that LRRK2 inhibition has the potential to inhibit interneuronal spread of tau pathology, slowing disease progression. Overall, pathways for tau entry share significant similarity with those required for virus entry by receptor-mediated endocytosis, suggesting that tau spreading is a quasi-infectious process.

INTRODUCTION

Dementias that involve the microtubule-associated protein tau (tau, MAPT), such as Alzheimer's disease, frontotemporal dementia and progressive supranuclear palsy, are referred to collectively as tauopathies[1]. Characterised by the formation of intracellular neurofibrillary tangles, or aggregates of tau protein, these diseases also display stereotyped spatiotemporal progressions through the central nervous system, including the cerebral cortex[2,3]. Different forms of these diseases first present with pathology in defined brain regions, before progressing through the brain[3]. The spatial progression of tau aggregation mirrors the connectivity of the central nervous system[4], and the involvement of different brain regions is reflected in neurological symptoms. A current working model for tauopathy progression is that pathogenic forms of tau, proposed to be oligomers or aggregates, are released from neurons containing protein aggregates and then taken up by synaptically-connected neurons, in which they then seed further tau aggregation and neuronal dysfunction[2].

There is considerable interest in identifying the molecular agents that mediate intercellular disease spreading and the biological mechanisms involved, including cell surface receptors. In addition to understanding disease pathogenesis, such insights are essential to the rational design of therapies to slow disease progression[5]. While the identity of the pathogenic tau species responsible for disease propagation remain unknown, progress has been made in understanding the mechanisms of cellular uptake of tau[2]. Cell surface heparan sulfate proteoglycans have been found to be necessary for cellular uptake of tau aggregates[6], and we and others have found that human neurons efficiently take up both monomeric and aggregated tau by overlapping but distinct mechanisms, consistent with dynamin-dependent receptor-mediated endocytosis[7,8]. Recent work has identified the low density lipoprotein receptor LRP1 as a major neuronal receptor for tau uptake via receptor-mediated endocytosis[9].

To define the cell biology of neuronal uptake of extracellular tau, we used whole-genome CRISPR knockout screens in human iPSC-derived neurons to identify genes and pathways required for neuronal uptake of tau protein. It is currently not known which forms of tau mediate pathogenic spreading of tauopathy between neurons[10], although oligomers or aggregates of either full length tau or fragments that include the microtubule-binding region are considered strong candidates[11]. Therefore, we designed whole genome CRISPR knockout screens[12] for genes required for neuronal uptake of full-length monomer and aggregates of tau[7], using human iPSC-derived excitatory neurons[13], the primary cell type affected by tau aggregation into neurofibrillary tangles *in vivo*[1].

RESULTS

FACS-based CRISPR knockout screens in human neurons to identify genes and pathways required for uptake of extracellular tau

We have previously found that aggregated and monomeric tau are taken up by human neurons by overlapping, but distinct pathways[7]. To identify and compare the cellular pathways by which monomeric and aggregated tau enter neurons, FACS-based assays were optimised to measure uptake of both forms of tau by human iPSC-derived cortical neurons (Figure 1; Supplementary Figure 1). To focus the screens on genes required specifically for tau uptake, and not general mechanisms of receptor-mediated endocytosis, assays were designed to measure uptake of transferrin and tau by the same neurons (Figure 1). Importantly, transferrin endocytosis does not alter tau uptake at a range of concentrations (Figure 1; Supplementary Figure 1).

For CRISPR knockout screens, cerebral cortex progenitor cells were generated from KOLF2 human iPSCs, constitutively expressing Cas9 from the AAVS1 locus, using our previously described methods (Supplementary Figure 1)[13,14]. A lentivirus library composed of 100,090 gRNAs, targeting 18,025 genes[12], was introduced by infecting cortical progenitor cells at an MOI of 0.3, and the progenitor cells subsequently differentiated to cortical excitatory neurons for 30 days (Figure 1).

To identify lentivirus-infected, guide RNA-expressing neurons that failed to take up tau but remained competent to endocytose transferrin, neurons were exposed to extracellular tau (labelled with Dylight-488) and transferrin (conjugated with Alexa-633) for either 4 or 5 hours, before being dissociated and fixed. Lentivirus-infected, gRNA-expressing neurons were gated and the populations of tau+ /transferrin+ and tau-/transferrin+ cells collected. Libraries of gRNAs were prepared and sequenced from each population, and replicate screens analysed to identify gRNAs enriched in neurons that failed to take up tau using the MAGeCK algorithm, reflecting genes whose loss of function resulted in reduced tau uptake[15].

Receptors and pathways required for neuronal uptake of monomeric tau

Duplicate screens for monomeric tau uptake were analysed using MAGeCK[15] to identify genes whose loss of function results in reduced neuronal tau uptake (Figure 2). Applying a significance cutoff of $p<0.01$ identified 214 genes required for tau uptake (Figure 2). Notably the low density lipoprotein receptor LRP1, which has been shown to act as a tau receptor[9], was one of the two highest ranked genes identified in the monomeric tau uptake screens, confirming the validity of the screens. The most highly ranked gene identified was *LRRK2*, a

large multifunctional protein that regulates diverse intracellular vesicle trafficking processes, mutations in which are a cause of autosomal dominant Parkinson's disease[16].

In addition to *LRRK2*, there was a notable number of genes encoding regulators of endocytosis required for monomeric tau uptake, including several AP2 subunits (*AP2M1*, *AP2S1*), dynamin-2 (*DNM2*), clathrin heavy chain (*CLTC*), *RAB7A*, *HGS* and PI3 kinase subunits C3 and R4. Several genes involved in endosomal sorting, such as *SNX16*, and specifically recycling of the LRP1 receptor were also required for monomeric tau uptake, including *SNX17*[17] and the LDL receptor chaperone *MESD*/*MESDC2*[18]. In addition, genes involved in lysosome and autophagosome biogenesis and acidification were prominent, including the vATPase subunit *ATP6V1D*, the vATPase assembly protein *VMA21*[19], and the autophagy regulating proteins UVRAG and ATG4A[20].

In addition to individual genes, gene ontology and pathway analyses of the set of genes required for tau uptake provides a useful overview of the cellular mechanisms required for tau uptake. Gene ontology and functional analysis of the set of genes above the empirical significance threshold of $p<0.01$ found significant enrichment in several categories related to receptor-mediated endocytosis, including lipoprotein particle receptor binding, the endocytic vesicle membrane and the CCC complex (Figure 2B). In terms of cellular localisation, genes required for monomeric tau uptake were significantly enriched in proteins that are localised to clathrin-coated vesicles, endosomes, including late endosomes, COPI vesicles and ER-Golgi transport (Figure 2C).

CRISPR screen identifies genes and pathways required for neuronal uptake of aggregated tau

Screens for human neuronal uptake of aggregated tau were carried out in triplicate and significantly enriched genes identified by MAGeCK analysis of the three screens in combination[15]. Using the same significance cutoff of $p<0.01$ as for analysis of the monomeric tau screen identified 228 genes required for aggregated tau uptake (Figure 3). *LRP1* did not reach that threshold ($p=0.024$), although highly ranked in the screen output (ranked gene 522/18019).

As for monomeric tau, genes required for neuronal uptake of aggregated tau include regulators of endocytosis, such as *EEA1*, *HGS* and the PI3 kinase subunits C3 and R4. Similarly, genes encoding vATPase subunits were required for aggregated tau uptake (*ATP6V0E2, ATP6V0D1, ATP6V0A1*), as were autophagy genes such as *GABARAPL1* and *UVRAG*. Several genes encoding proteins involved in intracellular vesicular trafficking were

also required for aggregated tau uptake, including the AP-1 and AP-3 complexes (*AP1G1, AP3S1*), and the COG complex that regulates retrograde trafficking within the Golgi[21] (four of the eight COG subunits: 1, 4, 7 & 8).

Gene ontology and functional analysis identified categories enriched in the set of genes required for aggregated tau uptake, including vacuolar acidification, ER to Golgi vesicle-mediated transport, COPI and II vesicle and the COG complex. In terms of cellular compartments, genes required for aggregated tau uptake code for proteins that are significantly enriched in the endosome, phagophore, late endosome, Golgi, ER and ER-Golgi transport (Figure 3C).

Monomeric and aggregated tau access neurons by receptor-mediated endocytosis dependent on LRP1 and LRRK2

The CRISPR screens used here to identify genes required for neuronal tau uptake are based on a chronic loss-of-function strategy, with all genes targeted in neural progenitor cells, and tau uptake assayed in terminally differentiated neurons approximately 30 days later. An advantage of this approach is that it identifies genes that are not essential for neuronal differentiation and viability, and thus pathways that could potentially be manipulated therapeutically *in vivo* to slow disease progression. To test whether acute inhibition of key proteins would also alter tau uptake, we used a live-imaging assay of neuronal tau uptake, using tau labelled with the pH-sensitive dye (pHrodo) that fluoresces in the low pH environments of the late endosome and lysosome (see Experimental Procedures for details).

LRP1 has recently been identified as a major tau receptor for both monomeric and oligomeric tau[9], and was one of the two most significant genes identified as required for monomeric tau entry. However, LRP1 was ranked lower for aggregated tau entry (ranked 522 of 18,019 genes; p=0.024) in the FACS-based screen. To test the dependency of monomeric and aggregated tau entry on interaction with LRP1, we used two different acute approaches to inhibiting tau-LRP1 interactions, combined with live-imaging of neuronal uptake of pHrodo-labelled tau.

Blockade of all LDL receptors by addition of the pan-LDL receptor chaperone RAP[22] reduced uptake of both monomeric and aggregated tau by approximately 50% (Figure 4). In separate experiments we simultaneously added pHrodo-tau and recombinant domain IV of LRP1, the region defined as binding tau[9], to the culture medium, before imaging tau uptake (Figure 4). As with RAP, the addition of the LRP1 fragment reduced uptake of both monomeric and

aggregated tau by approximately 50% (Figure 4), confirming LRP1as a major receptor for neuronal uptake of both monomeric and aggregated tau.

The large, multidomain protein encoded by *LRRK2* has multiple roles in endocytosis and vesicle trafficking[16]. CRISPR knockout of *LRRK2* in progenitor cells removes all LRRK2 function from that stage, through neuronal differentiation, and would be expected to cause considerable disruption of the endolysosome-autophagy system. Mutations in *LRRK2* that are causal for PD with tau aggregation[23] are concentrated in the kinase domain (e.g., G2019S) and have been shown to be activating or gain of kinase function mutations[24]. Therefore, to test the dependency of tau uptake on kinase activity, and ask whether acute inhibition would alter tau uptake, iPSC-derived neurons were treated with small molecule LRRK2 inhibitors for 3 hours before exposure to extracellular monomeric or aggregated tau (Figure 4C, D). Acute inhibition of LRRK2 kinase activity with two different small molecule inhibitors (GSK2578215A and MLi-2) reduced uptake of monomeric tau by between 50% and 70%. Inhibition of LRRK2 also reduced uptake of aggregated tau, but to a lesser degree of between 40 and 50%, which may contribute to why *LRRK2* was not identified in the CRISPR screen for aggregated tau uptake.

Two subunits of PI3-kinase, *PIK3C3* and *PIK3R4*, were identified as required for uptake of both monomeric and aggregated tau. *PIK3C3* (*VPS34*) is a catalytic subunit of several PI3K complexes involved in regulating multiple aspects of the endolysosome-autophagy system, including endosome trafficking[25]. PIK3R4 forms a complex with PIK3C3 and another protein required for tau uptake, UVRAG, that regulates endocytosis, endosomal trafficking and autophagy (together with Beclin-1 – referred to as class III PI3 kinase complex II[25]). Loss of three of the subunits of complex II of class III PI3K all leads to reduced tau uptake, suggesting that class III PI3K activity is required for tau uptake.

To test the role of PI3K in tau uptake, all PI3K activity in human neurons was acutely inhibited by wortmannin[26] administration before addition of extracellular tau (Figure 4C, D). Live imaging of pHrodo-tau uptake demonstrated that wortmannin reduced uptake of extracellular monomeric and aggregated tau in a dose-dependent manner (Figure 4), demonstrating the dependency of tau uptake on PI3K activity.

Monomeric and aggregated tau use similar mechanisms for neuronal entry

Given the clear overlap between the genes identified as required for monomeric or aggregated tau entry, and the finding that proteins identified as required for monomeric tau entry are also required for aggregated tau entry, the degree of similarity between the

mechanisms of neuronal uptake of both forms of tau was analysed at the levels of genes and protein complexes (Figure 5). To do so, we compared the gene sets identified above from the monomeric and aggregated tau entry, defined using the empirical threshold significance of $p<0.01$.

There was a significant overlap in individual genes identified by the screens for monomeric and aggregated tau uptake (hypergeometric test $p <.001$; Figure 5A), confirming the overall similarity of the mechanisms for neuronal uptake of each form of tau. Genes common to both screens included the COG complex member *COG4*, the three class III PI3K complex members discussed above (*PIK3C3, PIK3R4* and *UVRAG*), and the tyrosine kinase *HGS*, which is a known downstream effector of PI3 kinase, ESCRT component and regulator of endosome trafficking[27].

In addition to individual genes, genes that contribute to four protein complexes were significantly enriched (FDR <0.05) among combined hits of the monomeric and aggregated tau uptake screens (Figure 5B). These four were the Conserved Oligomeric Golgi (COG) complex, involved in vesicular trafficking within the Golgi, the vesicular ATPase that acidifies the lysosome and autophagosome, the PIK3C complex discussed above, and the CCC complex, which regulates endosomal recycling, including recycling of LDL receptors[28]. Together, these emphasise the role of the endolysosome in uptake of both forms of tau, including receptor recycling, which was confirmed by the enrichment of categories including endocytic vesicle membrane and pH reduction in the ontology analysis (Figure 5C) and the localisation of the proteins encoded by genes common to both screens in endosomes and lysosomes (Figure 5D).

Cellular mechanisms for tau uptake and processing

To generate a coherent understanding of the pathways of tau entry and processing with neurons, the non-redundant set of genes required for uptake of either monomeric or aggregated tau was analysed for known direct protein-protein interactions (Figure 6A). The combined set of 431 genes/proteins contained many known protein-protein interactions, which formed several discrete subnetworks (Figure 6A).

Within the network is a large subnetwork of endosomal and endocytosis proteins (Figure 6A), which includes clathrin heavy chain (CLTC), dynamin-2 (DNM2), EEA1 and AP2 subunits. This subnetwork is part of a larger set of interactions that includes RAB7A, LRRK2, PIK3C3 and PIK3R4, all of which have roles in regulating endocytosis and endosome trafficking[16,25]. Two other notable protein interaction networks/complexes in the dataset

regulate vesicle trafficking and endosome sorting. Multiple components of the CCC complex that regulates endosomal sorting and receptor recycling are required for tau uptake, including CCDC22, CCDC93 and three COMMD proteins (2, 3 and 10). There is also a subnetwork centred on the Golgi vesicle trafficking COG complex (5 of the 8 core COG proteins), which is involved in Golgi vesicle trafficking. Four subunits of the vacuolar ATPase (ATP6V1D, ATPV0A1, ATPV0D1, ATPV0E2), together with three accessory or assembly subunits of the complex, VMA21, TMED119 and CCDC115, are all required for tau uptake. Given that acidification of late endosomes and lysosomes is a key requirement for receptor recycling, disruption of that process is likely to have considerable impact on surface receptor number and composition[29].

LRRK2 is the most densely connected protein within the protein-protein interaction network, with RAB7A and clathrin heavy chain (CLTC) also in the top five most connected proteins (Figure 6B-D). LRRK2 interacts directly with both RAB7A and CLTC, as well as interacting indirectly via mutually-shared interactors. These include the adaptor complex subunit AP2M1, which interacts with each of LRRK2, RAB7A and CLTC (Figure 6B-D). Overall, the number and density of protein-protein interactions in the tau uptake network that mediate endocytosis, endolysosome function and vesicular traffic underscore the importance of receptor-mediated endocytosis for neuronal uptake of extracellular tau.

Neuronal uptake of extracellular tau shares functional similarities with receptor-mediated viral entry

Current models for tau-mediated propagation of pathology between neurons proposes that pathogenic forms of tau seed aggregation in receiving cells in the cytoplasm. Thus, following endocytosis, extracellular tau is likely to exit the endolysosome as part of its pathogenic mechanism. This echoes the life-cycle of many viruses, which use a variety of mechanisms to enter human cells, including receptor-mediated endocytosis and micropinocytosis[30], and thence to deliver genetic material to the cytoplasm or nucleus for replication. The host factors or genes that regulate the entry and life cycle of several viruses have been comprehensively studied using RNAi and CRISPR screens. These include the neurotropic Zika virus[31] and Influenza A[32], which enter cells via receptor-mediated endocytosis, and Ebola[33], which uses micropinocytosis.

To compare the biology of tau entry and processing with that of genes required for different viruses entry, the sets of genes identified in the screens here were compared with those reported for Ebola, Zika and Influenza A infection (Figure 7). Significant overlaps in the number of genes common to both the monomeric and aggregated tau screens were found

with those reported for Zika and Influenza A infection (Figure 7A), but not with Ebola infection (Figure 7A). Genes required for both tau entry and either Zika or Influenza A infection and replication are significantly enriched in genes encoding the vATPase or its assembly, the COG complex and intracellular vesicular trafficking, as reflected in the gene ontology enrichments (Figure 7B, C), with their encoded proteins enriched in proteins localised to the endosome, lysosome and Golgi network (Figure 7D, E). The overlap in routes of cell entry by viruses and tau protein, at the levels of both individual genes and cellular pathways, suggests that tau entry in disease spreading is a quasi-infectious process.

DISCUSSION

We report here the characterisation by whole genome CRISPR knockout screens of the pathways for extracellular tau uptake by human cortical excitatory neurons, the primary cell type affected in tauopathies. Independent screens for full length monomeric and heparin-aggregated tau avoided making assumptions about the forms and fragments of tau that are present in interstitial fluid in the CNS and of the forms that are competent to enter neurons, and provided a broad view of the mechanisms for tau entry to human neurons. Consistent with our previous findings[7], whole genome functional screens found that monomeric and aggregated tau are taken up by neurons by overlapping pathways, with some significant differences, most notably the dependency of aggregated tau uptake on protein glycosylation. The major mode of entry identified in this study for both monomeric and aggregated tau is LRRK2-regulated receptor-mediated endocytosis, which is perturbed by a variety of disruptions of the integrity of the endolysosome-autophagy system and intracellular vesicular transport between the Golgi and other cellular compartments.

This study confirmed that the low density lipoprotein receptor LRP1 is a primary receptor for both monomeric and aggregated tau in human neurons, as recently described[9]. The identification of *LRP1* as one of the top two ranked genes required for monomeric tau uptake is an important validation of the functional genetic approach taken here to understanding the cell biology of neuronal tau uptake. It is noteworthy that two different strategies for acutely inhibiting tau-LRP1 interactions, using the RAP chaperone and domain IV of LRP1, found that LRP1 mediates at least half of tau uptake in neurons. However, neither strategy completely blocked tau entry, suggesting the LRP1 may not be the sole receptor for tau entry.

CRISPR screens for uptake of monomeric and aggregated tau identified similar genes and pathways required for uptake of each form of the protein, but with some differences. Although the specific genes identified in each screen were not identical, there was a high degree of convergence of hits in protein complexes, organelles and cellular pathways, particularly in genes encoding proteins regulating later stages of intracellular trafficking and processing, beyond the early endosome, and more general intracellular vesicular trafficking. For each form of tau, key regulators of receptor-mediated endocytosis were identified at the level of endocytosis for monomeric tau (clathrin heavy chain and dynamin-2), and within early endosomes for aggregated tau (EEA1). The differences here in specific genes identified is unlikely to reflect alternative routes for cellular entry of the forms of tau, as we and others have previously shown that aggregated tau is also dependent on dynamin-2 for

neuronal uptake[7,8], although it was not identified in CRISPR knockout screens here, confirming that both forms are internalised via dynamin-dependent endocytosis.

Beyond the early endosome, tau uptake is highly dependent on class III PI3-kinase, which was confirmed by acute small molecule inhibition. Class III PI3K is a major regulator of both endosome recycling to the plasma membrane, as well as autophagy and phagocytosis[25], and its involvement highlights that perturbations of receptor recycling and of wider vesicular trafficking, including autophagy, results in a loss of neuronal capacity for tau uptake.

Alterations in receptor recycling is a well-characterised consequence of loss of function of proteins involved in endosome sorting and recycling[29]. We report here that loss of *SNX17* and all of the individual components of the CCDC22/CCDC93/COMMD complex (CCC complex) reduces neuronal uptake of tau. Given that a key cargo for SNX17-mediated recycling is LRP1[17], and that SNX17 interacts with the WASH/CCC complex[17], it is likely that one consequence of loss of each of these proteins is a reduction in plasma membrane levels of LRP1. Similarly, late endosome and lysosome acidification is essential for receptor recycling during the sorting process[34], and we find that loss of multiple vATPase subunits, as well as accessory subunits and assembly proteins, all reduce tau uptake.

In addition to perturbations of the endolysosome, disruption of vesicular trafficking within the neuron also reduces neuronal tau uptake. Loss of five of the eight members of the conserved oligomeric complex of the Golgi (COG complex) reduces neuronal tau uptake. Tau uptake has previously been shown to be mediated by plasma membrane heparan sulfate proteoglycans[6], and mutations in COG complex components result in congenital disorders of glycosylation in humans that have a wide spectrum of neurodevelopmental pathologies [21]. Two other genes required for aggregated tau uptake, *B3GALNT1* and *B3GNTL1,* encode glycosyltransferases[35]. Thus, it is likely that the loss of COGs and the glycosyltransferases both result in disruption of cell surface heparan sulfate proteoglycan assembly and thus reduced aggregated tau uptake.

The dependency of tau uptake on surface receptor expression, receptor-mediated endocytosis and wider homeostasis of intracellular vesicular trafficking has similarities with the host factors regulating viral entry and replication, particularly for viruses that enter human cells by receptor-mediated endocytosis. Comparing the results of this study with loss of function screens for viral entry, we find significant overlap in genes and protein complexes required in each case. This ranges from endocytosis, through vATPase activity to the COG and TRAPPC complexes in the Golgi. The similarities in the cell biology of the two processes

indicates that tau entry to neurons is a quasi-infectious process, which adapts normal cellular processes to both gain entry to the endolysosome and also to propagate within neurons.

Finally, the involvement of LRRK2 in tau uptake by human neurons resolves open questions about the role of LRRK2 in tauopathies. Missense, dominant mutations in *LRRK2* are a cause of familial Parkinson's disease (PD), and result in kinase activation, and LRRK2 variants are risk factors for sporadic PD[36]. PD due to *LRRK2* mutations is commonly accompanied by intraneuronal tau aggregation in the cerebral cortex[23]. Furthermore, missense *MAPT* mutations can cause both PD and FTD, and GWAS have identified *MAPT* variants as risk factors for PD[36]. Thus, both *LRRK2* and *MAPT* are associated with the pathogenesis of both sporadic and genetic forms of PD[36], with *LRRK2* mutations facilitating the development of tau pathology in PD and PD dementia.

In contrast, whereas tau is involved in Alzheimer's disease pathogenesis, and mutations in *MAPT*/tau are a cause of frontotemporal dementia[1], *LRRK2* mutations or variants are not associated with the development of tauopathies. However, recent GWAS for rate of progression of a tauopathy, progressive supranuclear palsy, identified variants in a putative enhancer for *LRRK2* that increase rate of progression[37]. We report here that LRRK2 is required for uptake of monomeric and aggregated tau by human neurons, indicating that LRRK2 mediates spreading of tau pathology in tauopathies, such as Alzheimer's disease. Furthermore, acute inhibition of the kinase activity of LRRK2 is sufficient to block neuronal tau uptake, demonstrating that LRRK2 is actively involved in mediated receptor-mediated endocytosis of extracellular tau. These findings suggest that small molecule inhibition of LRRK2 may have a role in slowing disease progression in neurodegenerative diseases involving spread of tau aggregation, including Alzheimer's disease.

EXPERIMENTAL PROCEDURES

Production and characterization of human iPSC-derived cerebral cortex neurons

Human pluripotent stem cell lines used in this study were KOLF2-C1 (WTSIi018-B-1) and derivative constitutively expressing Cas9 protein (KOLF2-C1 Cas9). KOLF2-C1 Cas9 was generated by integration of a Cas9 transgene driven by a CAGG promoter at the AAVS1 locus. Cells were nucleofected (Lonza) with recombinant enhanced specificity Cas9 protein (eSpCas9_1.1), a synthetic crRNA/tracrRNA (target site ggggccactagggacaggat tgg) and a homology directed repair template (https://www.addgene.org/86698/) followed by selection in neomycin (50 ug/ml) and clonal isolation[38]. Integrated clones were identified using PCR across the homology arms and validated by Sanger sequencing of the entire transgene and measurements of Cas9 activity. Random integration was screened for using PCR within the antibiotic resistance gene of the template plasmid.

Directed differentiation of human iPSCs to cerebral cortex was carried out as described, with minor modifications[13,14]. To establish identity and quality of neuronal induction, gene expression profiling was performed on a custom gene expression panel[39]. RNA was isolated from iPSC cortical inductions 35 days after induction, using an RNA extraction kit (QIAGEN). Expression of genes in neurons (MAP2, MAPT, and NGN2), cerebral cortex progenitor cells (EMX2, PAX6, and FOXG1), ventral telencephalon (NKX2-1 and LHX8), and mid-/hindbrain (HOXA and HOXB) was assessed in all neuronal inductions on the Nanostring nCounter platform. Immunofluorescent staining was performed on neurons as previously described[40] using the following primary antibodies: tau (Dako, A0024), MAP2 (abcam; ab5392) and Tuj1 (Cambridge Bioscience; ab14545). Secondary antibodies used were as follows: anti-mouse Alexa594 (A21125), goat anti-chicken Alexa 647 (A21449), goat anti-rabbit Alexa 546 (A11010, all from Thermo Fisher Scientific). Samples were stained with DAPI (1:5000 in PBS). Images were acquired through Olympus Inverted FV1000 confocal microscope and processed using the Fiji software[41].

Cas9 editing efficiency in human iPSC neurons

Knockout efficiency in KOLF2-C1 Cas9 neurons was assessed using a lentiviral reporter system[12]. Briefly, neurons were infected (30 days after induction) with lentiviruses expressing fluorophores mCherry and GFP and an sgRNA targeting GFP (pKLV2-U6gRNA(gGFP)-PGKmCherry2AGFP-W; modified from[12]. Neurons were dissociated (Accutase [Sigma, A6964]) 5, 12, 17 and 29 days after infection and analysed by flow cytometry (SH800S Cell Sorter, Sony). Knockout efficiency was calculated as the ratio of

mCherry positive, GFP negative neurons over total infected cells (mCherry positive, GFP positive and negative) (FlowJo software).

Genome-wide CRISPR RNA guide lentiviral library

The Human CRISPR Library v.1.1 was used in this study. The Human CRISPR Libraries v.1.0 and v1.1 have been previously described (Addgene, 67989)[12,42]. CRISPR Library v.1.1 contains all the guides from v1.0 targeting 18,009 genes with 90,709 sgRNAs, plus five additional sgRNAs against 1,876 selected genes[43]. Lentiviruses were produced by transfecting HEK 293 cells with lentiviral vectors together with packaging vectors (3rd generation) using Lipofectamine 3000 (Thermofisher). Viral supernatant was collected 24hr and 48hr post-transfection, filtered, concentrated by centrifugation and stored at -80°C. The library was sequenced to assess the distribution of the guides. Virus MOI was determined by flow cytometry (SH800S Cell Sorter, Sony; FlowJo software). For each whole-genome CRISPR knockout screen, 4-6×10^7 neurons (35 days after induction) were transduced with an appropriate volume of the lentiviral packaged whole-genome sgRNA library to achieve 30-40% transduction efficiency (>100×library coverage).

Recombinant tau monomer and aggregate preparation

Recombinant tau protein was purified as previously described[7]. Briefly, tau P301S_FLAG×3_10×his-tag was overexpressed using the pET24d plasmid in BL21(DE3) bacteria (37°C, 50mg.mL^{-1} Kanamycin, IPTG 0.4mM). Cells were lysed (Avestin Emulsiflex C5) in lysis/binding buffer (20mM phosphate [pH7.4], 500mM NaCl, 20mM imidazole, protease inhibitor cocktail [Roche]), clarified lysate was applied to a 5mL HisTrapHP column (GE Healthcare) and washed with 10CV of lysis/binding buffer. Tau was eluted in 20mM phosphate (pH7.4), 500mM NaCl, 500mM imidazole. Peak fractions were pooled and further purified using a Superdex 200 16/60 gel filtration column (GE Healthcare) in 50mM phosphate (pH7.4), 150mM NaCl. Pooled fractions were then concentrated to approximately 8 mg/mL using a spin concentrator (Millipore). Tau aggregates were produced using 1mL tau P301S at 8mg/mL was incubated with 4 mg.mL^{-1} heparin (Sigma) in PBS plus 30 mM 3-(N-morpholino)propanesulfonic acid (MOPS) (pH 7.2) at 37°C for 72 hr. Aggregated material was diluted in 9 mL PBS plus 1% (v/v) sarkosyl (Sigma) and left rocking for 1 hr at room temperature to completely solubilize any non-aggregated material. Insoluble tau was pelleted by ultracentrifugation for 1hr at 4°C. The pellet was resuspended in 1mL PBS by vigorous pipetting and sonicated at 100W for 3×20s (Hielscher UP200St ultrasonicator) to disperse clumps of protein and break large filaments into smaller species. Final protein concentration was determined by BCA protein assay (BioRad).

To label purified recombinant tau (monomeric or aggregated tau P301S) with Dylight 488 NHS ester (Thermo Fisher Scientific) or pH-sensitive form of rhodamine (pHrodo, Thermo Fisher Scientific), 150 μM tau protein (or equivalent protein concentration for aggregate; ~7 $\mu g.mL^{-1}$) was incubated with either a 10 fold-molar excess of Dylight ($10mg.mL^{-1}$; dissolved in DMF) or pHrodo (10mM; dissolved in DMSO; with 10 fold molar excess of tris[2-carboxyethyl]phosphine; TCEP) for 2hrs in the dark at room temperature. After incubation, labelled protein samples were subjected to size exclusion chromatography at 4°C (Superdex 200 Increase 10/300 GL, GE Healthcare) in 50 mM phosphate (pH 7.4) and 150 mM NaCl to remove unreacted dye and assess perturbation of oligomeric state by labelling (no change was observed, data not shown). 64.5μM Transferrin from Human Serum, Alexa Fluor™ 633 Conjugate **(**T23362; Thermo Fisher Scientific) was dissolved in PBS.

Flow cytometry-based whole-genome screen for genes modifying tau entry and processing
Neurons infected with the Human CRISPR library were matured in neuronal maintenance medium (N2B27; media changed every two days) for 65 days. 24hrs prior to acute incubation with labelled recombinant proteins, media was exchanged to DMEM plus supplements (500ml DMEM/F-12 + GlutaMAX, 5mL N2 Supplement, 0.25mL Insulin ($4mg.mL^{-1}$), 1mL 2-Mercaptoethanol (50mM), 5mL MEM Non-Essential Amino Acids Solution, 5mL Sodium pyruvate (100mM) and 2.5mL Penicillin-Streptomycin (10,000 U/mL); ThermoFisher) to remove transferrin from the culture medium. The following day neurons were incubated with 30nM of transferrin-Alexa 633 and either 90nM monomeric or 400nM aggregated tau-Dylight for 4 or 5hrs, respectively. After two PBS washes, neuronal cultures were dissociated with papain (Worthington biochemical Corporation) supplemented with Accutase (Sigma, A6964) into single cells.

Dissociated neurons were collected by low-speed centrifugation (600×*g* for 15min), the supernatant was removed, filtered (Sysmex/Partec CellTrics 50μm filter) and fixed using 2% paraformaldehyde in PBS for 15min at room temperature. Neurons were washed twice in PBS, resuspended in PBS, 7.5% w/v BSA, 2mM EDTA and analysed and collected using a BD Influx cell sorter. Neurons were gated using forward and side scatter channels to isolate the viable cell population and exclude noise/debris, subsequently gated on forward scatter and trigger pulse width channel to isolate singlets then gated for fluorescence in the channels corresponding to BFP (sgRNA library), Dylight 488 (tau) and Alexa 633 (transferrin), using uninfected neurons and neurons without acute incubation of recombinant proteins to establish thresholds. Neuronal populations were collected that were positive for the sgRNA library and had high levels of labelled transferrin and either high or low levels of labelled tau protein. Flow cytometry data were analysed using FlowJo software.

Guide RNA sequencing

Genomic DNA was extracted from cell pellets using QuickExtract DNA Extraction Solution (Cambio; QE09050) as per the manufacturer's instructions. sgRNA amplification was performed using a two-step PCR strategy and purified using Agencourt AMPure XP (A63880; Beckman Coulter UK), Illumina sequencing (19-bp single-end sequencing with custom primers on the HiSeq2500 Rapid Run) and sgRNA counting were performed as described previously[12].

CRISPR screen data analysis

sgRNA count files from purified neuronal populations that had high levels of labelled transferrin and tau were compared to neuronal populations with high levels of labelled transferrin and low levels of labelled tau protein using MAGeCK (0.5.8)[15]. Replicate monomeric (n=2) and aggregated (n=3) tau uptake screens were analysed separately. sg-RNA rankings were summarised into gene-level statistics using the RRA algorithm. All subsequent analyses were performed in R[44]. For genes with two sets of sgRNAs, the higher ranking set was kept and the lower ranking set was discarded. An empirical threshold of unadjusted p-value < 0.01 was used to identify genes required for tau uptake in either screen, identifying 214 genes in the aggregated screen and 228 genes in the monomeric screen. Functional term enrichment analysis was performed using gProfiler 2 querying the GO, REAC, and CORUM databases[45].

Compartment localisation enrichment was performed using localisation scores from the COMPARTMENTS database[46]. Localisation of each gene to a particular compartment is given a score up to 5 based on the strength of the supporting evidence. To calculate compartment localisation enrichment for the genes identified in the CRISPR screens, a gene set localisation score for each compartment was calculated by averaging the localisation score of all constitutive genes. The score ranged from 0 to 1, with 1 representing maximum localisation score for that compartment for all the genes in the set. Cellular compartments were removed from analysis if too undescriptive (gene-set localisation score >= 0.7), with low signal (gene-set localisation score <= 0.02), or with only weak evidence (no individual gene scoring 3.5/5 or above). Compartment localisation enrichment was calculated compared to the mean value obtained from 100,000 simulated random sets of 221 (aggregated, monomeric screens) or 431 (combined aggregated and monomeric), 15 (influenza A and combined aggregated and monomeric), or 8 (Zika and combined aggregated and monomeric) genes represented in the CRISPR library. Boot-strapping was used to calculate p-values and significance was adjusted for multiple comparison using false

discovery rate. For significantly enriched compartments, the log2 fold-change of compartment score over random was mapped onto a diagram of cellular compartments using the sp package[47].

Protein-protein interaction networks were constructed using the PSICQUIC package using the following databases: BioGrid, bhf-ucl, IntAct, MINT, UniProt, MBInfo, InnateDB[48]. All PPIs for the human proteins were maintained, removing reciprocal and self interactions. Network graphs were drawn using igraph and visNetwork packages[49].

Live imaging of tau entry and processing by human iPSC neurons

Neurons grown (65 days after induction) on 96-well plates (CellCarrier96; Perkin Elmer Life Sciences; 6055308) were imaged for fluorescent pHrodo-labelled tau protein (excitation at 577nm and emission at 641nm in an acidic environment) using a 20× IncuCyte S3 Live-cell Analysis System (Sartorius). Bright-field and fluorescence emission images were collected at 45min or 1hr intervals for 16hrs at 37°C. Parameters for fluorescent objects were set (fluorescent intensity and contrast), quantified and intensity of the field was normalised to confluency using the Incucyte Analysis Software. Data were analysed using Prism Software (GraphPad). Typically, conditions were repeated at least in triplicate and nine fields recorded per well.

Live imaging assays were performed using monomeric (50nM) or aggregated (100nM, equivalent calculated from monomeric tau; 5ug.mL^{-1}) pHrodo-labelled tau. For competitive binding experiments, recombinant peptides were resuspended in PBS, and PBS was the vehicle control in experiments. Recombinant proteins were separately preincubated with neuronal cultures and recombinant tau protein for 3 hours prior to incubation of neuronal cultures with the mixer containing recombinant proteins (100nM Human LRP-1 Cluster IV Fc Chimera Protein; 10nM Human LRPAP Protein [R&D systems]). For pharmacological treatments, compounds were dissolved in DMSO at the concentrations noted, and DMSO was the vehicle control in experiments. Compounds were added 3 hours prior to incubation with recombinant tau protein (LRRK2 inhibitor (1): GSK2578215A; LRRK2 inhibitor (2): MLi-2; Wortmanin [Tocris Bioscience]). neurotoxicity/neurolysis were assessed by analysing the level of lactate dehydrogenase (LDH) activity (Roche; 11644739001) in conditioned media samples following treatments.

Statistical Analysis

The number of replica wells and experiments are indicated in the figure legends for each assay where appropriate. For live-cell imaging assays using pHrodo-labeled protein,

intensity normalised to confluence of the field using the Incucyte Analysis Software. Typically, 9 fields were recorded per well and an average generated from the Incucyte Analysis Software. Analyses were performed using the Prism version 8 software (GraphPad). One-way ANOVA with Dunnett's multiple testing or Student's t test was used where appropriate.

Hypergeometric tests were used to evaluate significance of overlap between gene sets. Genes required for uptake of Ebola, influenza A, and Zika viruses were obtained from published CRISPR screens[31–33]. Since the Ebola data were also analysed with MAGeCK, we defined genes required for viral uptake using an unadjusted p-value threshold of 0.01; this information was not available for the influenza A and Zika studies, so we defined genes required for viral uptake as having an adjusted p-value < 0.05. Hypergeometric tests for overlap in screen hits were carried out using the set of genes analysed in both studies as background.

ACKNOWLEDGEMENTS

The authors thank Sarah Spain, Paris Litterick, Alison Mann, David Hulcoop and Ian Dunham of the Open Targets team at the European Bioinformatics Institute and Wellcome Sanger Institute for ongoing support of this research; Chun-Fang Xu (GSK) and Jinkuk Choi (Biogen) for feedback on data interpretation; Sam Thompson, Jennie Graham, Chris Hall and Bee Ling Ng for flow cytometry support (Sanger Institute); and Tom Campbell, Sergey Sitnikov and Clare Jones for technical assistance (Talisman Therapeutics).

FUNDING

This work was funded by Open Targets (OTAR036, www.opentargets.org). This research was also supported by Wellcome (Investigator Award to FJL), Alzheimer's Research UK (Stem Cell Research Centre), Dementias Platform UK (Stem Cell Network) and Great Ormond Street Hospital Charity.

COMPETING INTERESTS

Open Targets is a public–private partnership between non-profit research institutions and the pharmaceutical industry.

REFERENCES

1. Lee, V. M.-Y., Goedert, M. & Trojanowski, J. Q. Neurodegenerative Tauopathies. *Annu. Rev. Neurosci.* **24**, 1121–1159 (2001).
2. Goedert, M., Eisenberg, D. S. & Crowther, R. A. Propagation of Tau Aggregates and Neurodegeneration. *Annu. Rev. Neurosci.* **40**, 189–210 (2017).
3. Braak, H. & Braak, E. Neuropathological stageing of Alzheimer-related changes. *Acta Neuropathol. (Berl.)* **82**, 239–259 (1991).
4. Vogel, J. W. *et al.* Spread of pathological tau proteins through communicating neurons in human Alzheimer's disease. *Nat. Commun.* **11**, 2612 (2020).
5. Colin, M. *et al.* From the prion-like propagation hypothesis to therapeutic strategies of anti-tau immunotherapy. *Acta Neuropathol. (Berl.)* **139**, 3–25 (2020).
6. Bb, H. *et al.* Heparan sulfate proteoglycans mediate internalization and propagation of specific proteopathic seeds. *Proceedings of the National Academy of Sciences of the United States of America* vol. 110 https://pubmed.ncbi.nlm.nih.gov/23898162/ (2013).
7. Evans, L. D. *et al.* Extracellular Monomeric and Aggregated Tau Efficiently Enter Human Neurons through Overlapping but Distinct Pathways. *Cell Rep.* **22**, 3612–3624 (2018).
8. Rauch, J. N. *et al.* Tau Internalization is Regulated by 6-O Sulfation on Heparan Sulfate Proteoglycans (HSPGs). *Sci. Rep.* **8**, 6382 (2018).
9. Rauch, J. N. *et al.* LRP1 is a master regulator of tau uptake and spread. *Nature* **580**, 381–385 (2020).
10. Kaniyappan, S. *et al.* FRET-based Tau seeding assay does not represent prion-like templated assembly of Tau fibers. *bioRxiv* 2020.03.25.998831 (2020) doi:10.1101/2020.03.25.998831.
11. Walsh, D. M. & Selkoe, D. J. A critical appraisal of the pathogenic protein spread hypothesis of neurodegeneration. *Nat. Rev. Neurosci.* **17**, 251–260 (2016).
12. Tzelepis, K. *et al.* A CRISPR Dropout Screen Identifies Genetic Vulnerabilities and Therapeutic Targets in Acute Myeloid Leukemia. *Cell Rep.* **17**, 1193–1205 (2016).

13. Shi, Y., Kirwan, P., Smith, J., Robinson, H. P. C. & Livesey, F. J. Human cerebral cortex development from pluripotent stem cells to functional excitatory synapses. *Nat. Neurosci.* **15**, 477–486, S1 (2012).

14. Shi, Y., Kirwan, P. & Livesey, F. J. Directed differentiation of human pluripotent stem cells to cerebral cortex neurons and neural networks. *Nat. Protoc.* **7**, 1836–1846 (2012).

15. Li, W. *et al.* MAGeCK enables robust identification of essential genes from genome-scale CRISPR/Cas9 knockout screens. *Genome Biol.* **15**, 554 (2014).

16. Taylor, M. & Alessi, D. R. Advances in elucidating the function of leucine-rich repeat protein kinase-2 in normal cells and Parkinson's disease. *Curr. Opin. Cell Biol.* **63**, 102–113 (2020).

17. McNally, K. E. *et al.* Retriever is a multiprotein complex for retromer-independent endosomal cargo recycling. *Nat. Cell Biol.* **19**, 1214–1225 (2017).

18. Hoshi, T. *et al.* Mesdc2 plays a key role in cell-surface expression of Lrp4 and postsynaptic specialization in myotubes. *FEBS Lett.* **587**, 3749–3754 (2013).

19. Hill, K. J. & Stevens, T. H. Vma21p is a yeast membrane protein retained in the endoplasmic reticulum by a di-lysine motif and is required for the assembly of the vacuolar H(+)-ATPase complex. *Mol. Biol. Cell* **5**, 1039–1050 (1994).

20. Liang, C., Feng, P., Ku, B., Oh, B.-H. & Jung, J. U. UVRAG: a new player in autophagy and tumor cell growth. *Autophagy* **3**, 69–71 (2007).

21. D'Souza, Z., Taher, F. S. & Lupashin, V. V. Golgi inCOGnito: From vesicle tethering to human disease. *Biochim. Biophys. Acta Gen. Subj.* 129694 (2020) doi:10.1016/j.bbagen.2020.129694.

22. Herz, J., Goldstein, J. L., Strickland, D. K., Ho, Y. K. & Brown, M. S. 39-kDa protein modulates binding of ligands to low density lipoprotein receptor-related protein/alpha 2-macroglobulin receptor. *J. Biol. Chem.* **266**, 21232–21238 (1991).

23. Henderson, M. X., Sengupta, M., Trojanowski, J. Q. & Lee, V. M. Y. Alzheimer's disease tau is a prominent pathology in LRRK2 Parkinson's disease. *Acta Neuropathol. Commun.* **7**, 183 (2019).

24. West, A. B. *et al.* Parkinson's disease-associated mutations in leucine-rich repeat kinase 2 augment kinase activity. *Proc. Natl. Acad. Sci. U. S. A.* **102**, 16842–16847 (2005).

25. Bilanges, B., Posor, Y. & Vanhaesebroeck, B. PI3K isoforms in cell signalling and vesicle trafficking. *Nat. Rev. Mol. Cell Biol.* **20**, 515–534 (2019).

26. Cuenda, A. & Alessi, D. R. Use of kinase inhibitors to dissect signaling pathways. *Methods Mol. Biol. Clifton NJ* **99**, 161–175 (2000).

27. Raiborg, C. & Stenmark, H. The ESCRT machinery in endosomal sorting of ubiquitylated membrane proteins. *Nature* **458**, 445–452 (2009).

28. Bartuzi, P. *et al.* CCC- and WASH-mediated endosomal sorting of LDLR is required for normal clearance of circulating LDL. *Nat. Commun.* **7**, 10961 (2016).

29. Cullen, P. J. & Steinberg, F. To degrade or not to degrade: mechanisms and significance of endocytic recycling. *Nat. Rev. Mol. Cell Biol.* **19**, 679–696 (2018).

30. Thorley, J. A., McKeating, J. A. & Rappoport, J. Z. Mechanisms of viral entry: sneaking in the front door. *Protoplasma* **244**, 15 (2010).

31. Li, Y. *et al.* Genome-wide CRISPR screen for Zika virus resistance in human neural cells. *Proc. Natl. Acad. Sci. U. S. A.* **116**, 9527–9532 (2019).

32. Li, B. *et al.* Genome-wide CRISPR screen identifies host dependency factors for influenza A virus infection. *Nat. Commun.* **11**, 164 (2020).

33. Flint, M. *et al.* A genome-wide CRISPR screen identifies N-acetylglucosamine-1-phosphate transferase as a potential antiviral target for Ebola virus. *Nat. Commun.* **10**, 285 (2019).

34. McNally, K. E. & Cullen, P. J. Endosomal Retrieval of Cargo: Retromer Is Not Alone. *Trends Cell Biol.* **28**, 807–822 (2018).

35. Ricci Hagman, J., Westman, J. S., Hellberg, Å. & Olsson, M. L. An update on the GLOB blood group system (and former GLOB collection). *Immunohematology* **34**, 161–163 (2018).

36. Hardy, J. Genetic analysis of pathways to Parkinson disease. *Neuron* **68**, 201–206 (2010).

37. Jabbari, edwin. Common variation at the LRRK2 locus is associated with survival in the primary tauopathy progressive supranuclear palsy | bioRxiv. https://www.biorxiv.org/content/10.1101/2020.02.04.932335v1.

38. Bruntraeger, M., Byrne, M., Long, K. & Bassett, A. R. Editing the Genome of Human Induced Pluripotent Stem Cells Using CRISPR/Cas9 Ribonucleoprotein Complexes. *Methods Mol. Biol. Clifton NJ* **1961**, 153–183 (2019).

39. A, S., E, T., Ve, S. & Fj, L. Variable Outcomes in Neural Differentiation of Human PSCs Arise from Intrinsic Differences in Developmental Signaling Pathways. *Cell reports* vol. 31 https://pubmed.ncbi.nlm.nih.gov/32521257/ (2020).

40. Moore, S. *et al.* APP metabolism regulates tau proteostasis in human cerebral cortex neurons. *Cell Rep.* **11**, 689–696 (2015).

41. J, S. *et al.* Fiji: an open-source platform for biological-image analysis. *Nature methods* vol. 9 https://pubmed.ncbi.nlm.nih.gov/22743772/ (2012).

42. Fm, B. *et al.* Prioritization of cancer therapeutic targets using CRISPR-Cas9 screens. *Nature* vol. 568 https://pubmed.ncbi.nlm.nih.gov/30971826/ (2019).

43. Wang, T., Wei, J. J., Sabatini, D. M. & Lander, E. S. Genetic screens in human cells using the CRISPR-Cas9 system. *Science* **343**, 80–84 (2014).

44. R Core Team. *R: A Language and Environment for Statistical Computing*. (R Foundation, 2020).

45. Raudvere, U. *et al.* g:Profiler: a web server for functional enrichment analysis and conversions of gene lists (2019 update). *Nucleic Acids Res.* **47**, W191–W198 (2019).

46. Binder, J. X. *et al.* COMPARTMENTS: unification and visualization of protein subcellular localization evidence. *Database* **2014**, (2014).

47. Renard, D. Roger S. Bivand, Edzer J. Pebesma, Virgilio Gomez-Rubio: Applied Spatial Data Analysis with R: Springer, New York, 2008. 378 pp. ISBN 978-0-387-78170-9. *Math. Geosci.* **43**, 607–609 (2011).

48. Aranda, B. *et al.* PSICQUIC and PSISCORE: accessing and scoring molecular interactions. *Nat. Methods* **8**, 528–529 (2011).

49. Almende, B. V., Thieurmel, B. & Robert, T. visNetwork: Network Visualization using 'vis.js' Library. R package version 2.0.9.

FIGURES AND LEGENDS

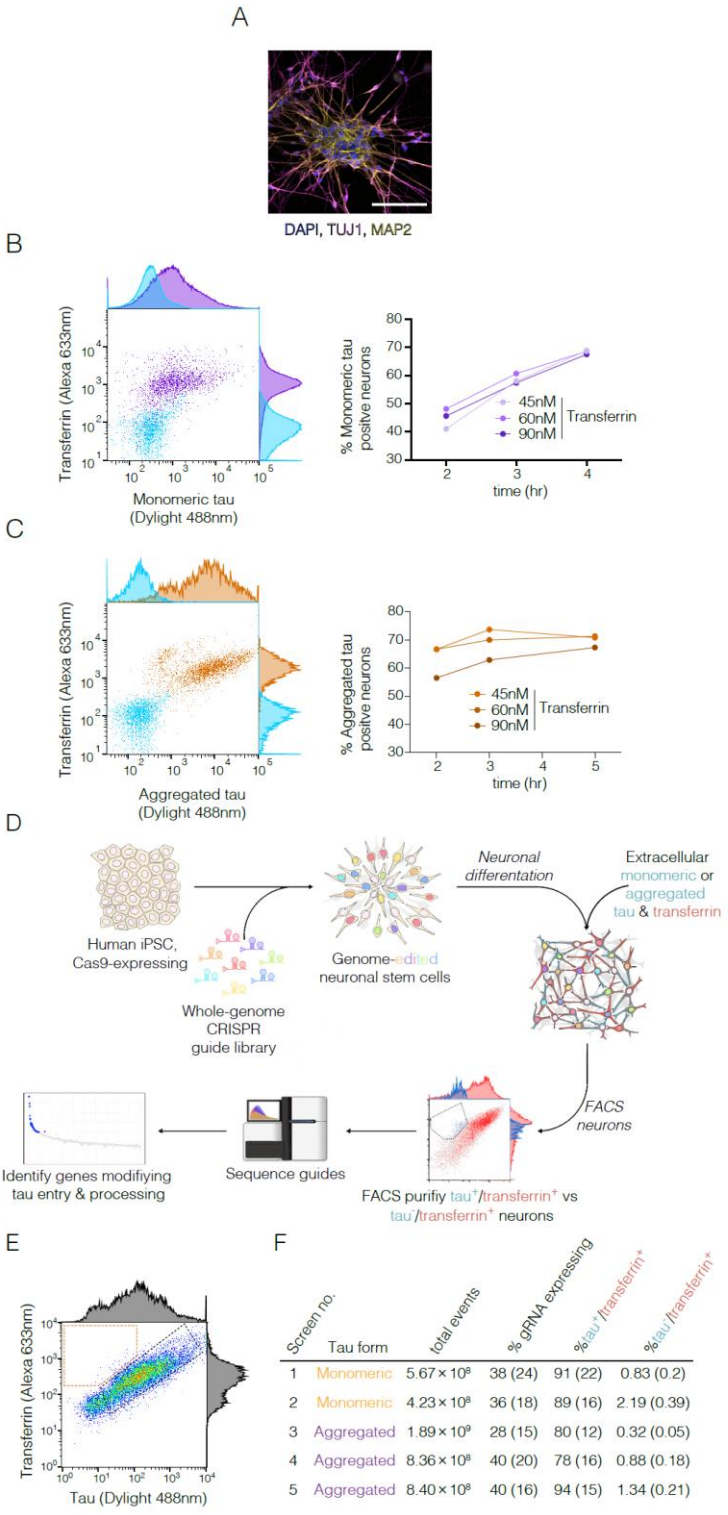

Screen no.	Tau form	total events	% gRNA expressing	%tau+/transferrin+	%tau-/transferrin+
1	Monomeric	5.67×10^8	38 (24)	91 (22)	0.83 (0.2)
2	Monomeric	4.23×10^8	36 (18)	89 (16)	2.19 (0.39)
3	Aggregated	1.89×10^9	28 (15)	80 (12)	0.32 (0.05)
4	Aggregated	8.36×10^8	40 (20)	78 (16)	0.88 (0.18)
5	Aggregated	8.40×10^8	40 (16)	94 (15)	1.34 (0.21)

Figure 1: FACS-based CRISPR knockout screens in human neurons to identify genes and pathways required for uptake of extracellular tau

A. Neuronal identity of differentiated human (KOLF2 C1) iPSC-derived cortical excitatory neurons fixed human iPSC-derived neurons (35 days after induction) were co-stained with

DAPI (nuclear DNA; blue), TUJ1 (neuronal; magenta) and MAP2 (neuronal dendrites and cell bodies; yellow). Confocal microscopy representative image is shown. Scale bar, 100μm.

B,C. Transferrin does not compete with or alter extracellular tau entry or processing in neurons. Human iPSC-derived neurons (65 days after induction) were incubated with 20nM monomeric (**B**; purple) or 400nM aggregated (**C**; orange) tau protein (Dylight 488 labelled) and transferrin (Alexa 633 conjugate; concentrations indicated), neurons were dissociated into single cells at indicated time points and analysed by flow cytometry. Scatterplots of tau-Dylight/transferrin-Alexa double-labelled neurons were gated by forward and side scatter and subsequently by transferrin-Alexa and tau-Dylight fluorescence. Neurons without tau or transferrin incubation (light blue) were used to establish the threshold level for detection of tau-Dylight fluorescence. Percentage of monomeric or aggregated tau positive neurons at indicated transferrin concentrations plotted against time after protein incubation initiation.

D. Design of whole genome CRISPR knockout screens for uptake of tau by human iPSC-derived neurons. Following neuronal induction of iPSC stem cells, a lenti-viral whole-genome CRISPR-Cas9 sgRNA library was infected into neuronal stem cells. Neurons were maintained in culture for 65 days. Gene-edited neurons were exposed to extracellular, fluorophore-labelled tau and transferrin (4-5hrs), following which they were disassociated to single cells, fixed, sorted and purified using flow cytometry for neurons infected with sgRNA, abd that had high levels of transferrin (+) and either high (+) or low (-) levels of tau. Following extraction of genomic DNA from each collected population of neuron, sgRNAs were sequenced compared using MAGeCK algorithm to identify genes that modify tau entry and processing, without affecting transferrin uptake.

E. Scatter plot of FACS analysis of population of neurons from typical screen outcome, highlighting neurons expressing gRNAs (gated on BFP signal) that are tau-negative but transferrin-positive (dashed orange line) and tau-positive and transferrin-positive (dashed black line).

F. Summary of the CRISPR screens reported here for tau uptake, including numbers of cells analysed and proportion of neurons exhibiting reduced tau uptake as a proportion of gRNA expressing cells. Figures in brackets are the percentages of the total events.

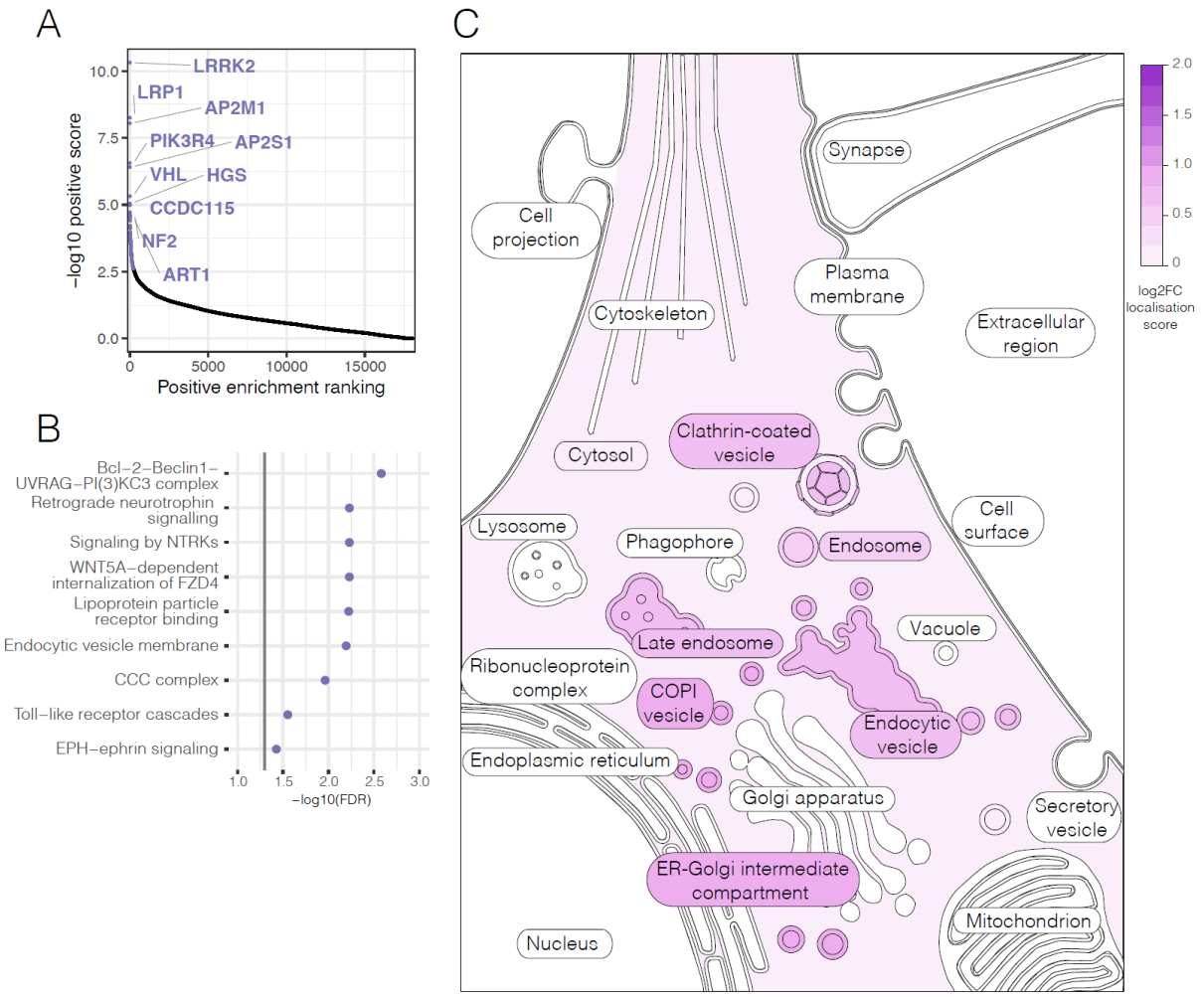

Figure 2: CRISPR screen identifies genes and pathways required for neuronal uptake of monomeric tau

A. Whole-genome enrichment score and ranking in comparison of transferrin+/tau- *vs* transferrin+/tau+ neuronal populations in knockout screen for monomeric tau uptake (2 repeats). Using a p-value cut-off of 0.01, 214 genes were identified as required for monomeric tau uptake (purple points). The 10 highest scoring genes are labelled.

B. Functional annotations enriched among 214 genes required for monomeric tau uptake (representative selection).

C. Genes required for monomeric tau uptake code for proteins with a significantly higher than random localisation score in particular cellular compartments in the COMPARTMENTS dataset (FDR < 0.05). Significantly enriched compartments are coloured based on the strength of enrichment (log2 fold-change) whereas non-significant compartments are left white.

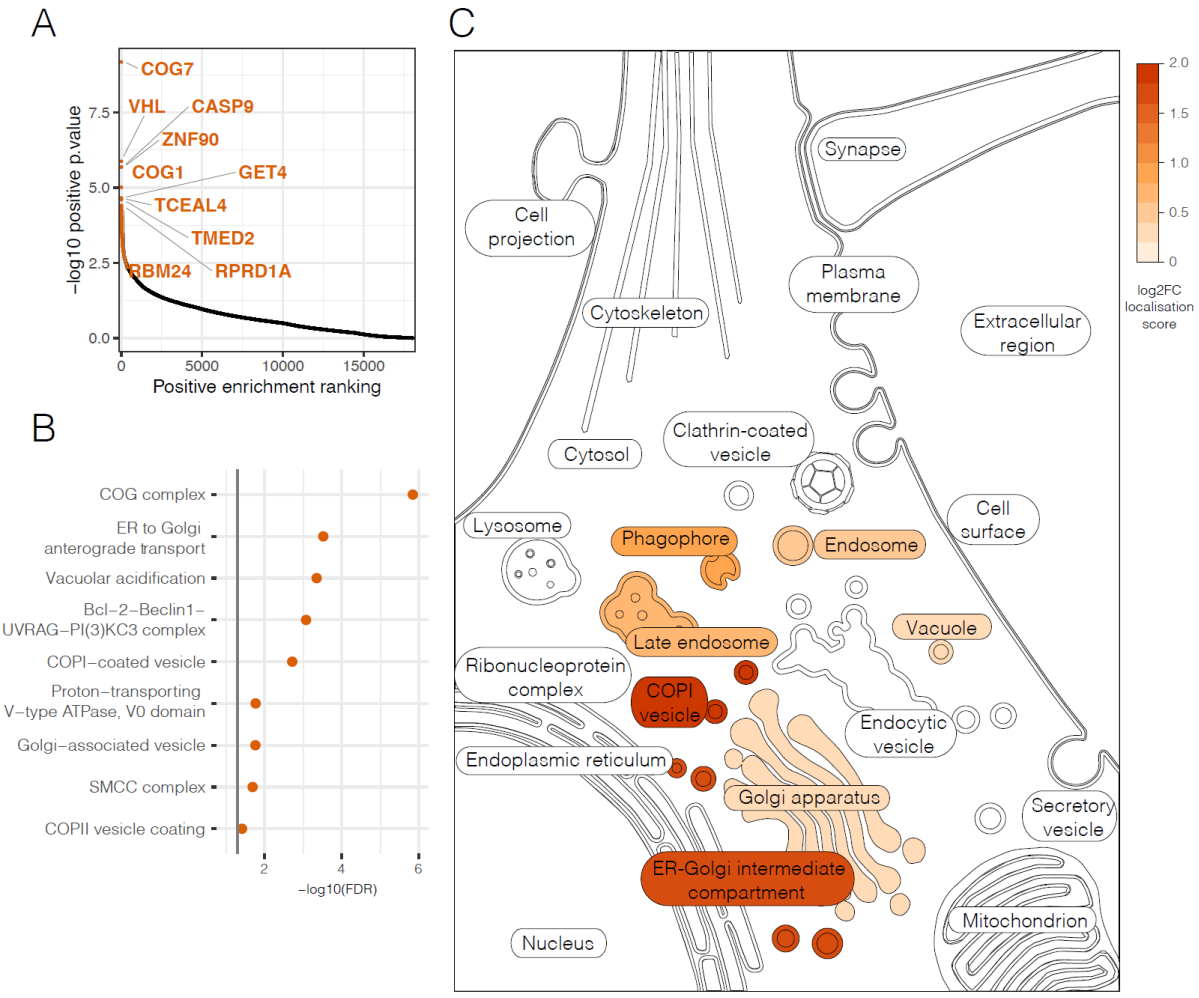

Figure 3: CRISPR loss of function screens identify genes and pathways required for neuronal uptake of aggregated tau

A. Whole-genome enrichment score and ranking in comparison of transferrin+/tau- *vs* transferrin+/tau+ neuronal populations in knockout screen for aggregated tau uptake (3 repeats). Using a p-value cut-off of 0.01, 228 genes were identified as required for aggregated tau uptake (orange points). The 10 highest scoring genes are labelled.

B. Functional annotations enriched among 228 genes required for aggregated tau uptake.

C. Genes required for aggregated tau uptake code for proteins with a significantly higher than random localisation score in particular cellular compartments in the COMPARTMENTS dataset (FDR < 0.05). Significantly enriched compartments are coloured based on the strength of enrichment (log2 fold-change) whereas non-significant compartments are left white.

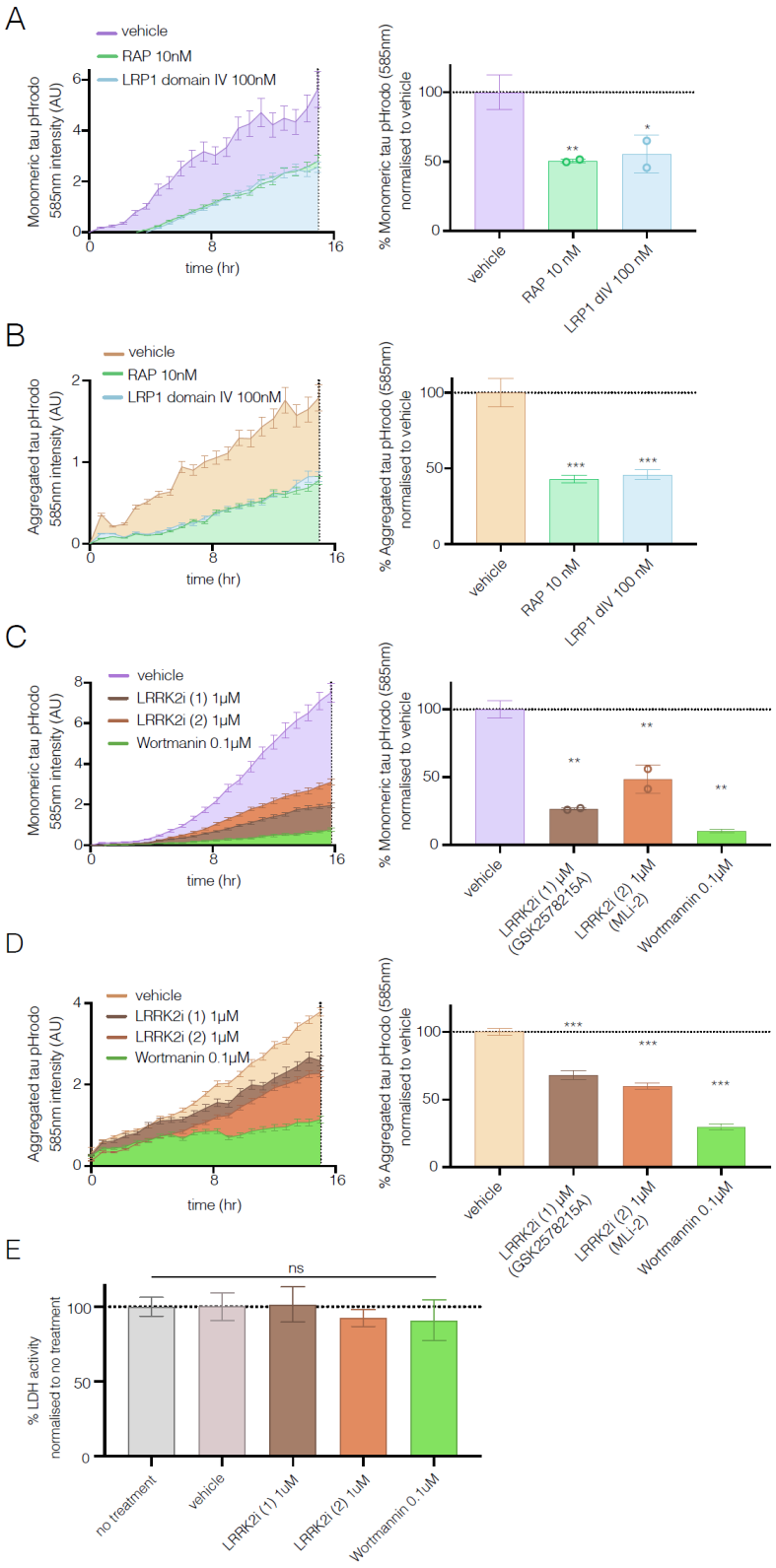

Figure 4: Monomeric and aggregated tau access neurons by receptor-mediated endocytosis dependent on LRP1, LRRK2 and PI3-kinase

(**A,B**) Uptake of pHrodo-labelled monomeric (A) and aggregated (B) tau is mediated by LRP1, and blocked. pHrodo-tau was preincubated with either 10nM RAP, 100nM Human LRP-1 Cluster IV Fc chimera protein or vehicle control (PBS) for 3hrs prior to addition to

extracellular media and live imaging of neuronal uptake of tau. Histograms report tau uptake at final timepoint, which was significantly reduced by both treatments, and for monomeric and aggregated tau. Minimum of 3 wells per treatment, and average of 9 fields of view per well. Error bars indicate SD. Significance was determined using one-way ANOVA (n = 3; $^{*}p < 0.05$, $^{**}p < 0.005$, and $^{***}p < 0.0001$, Dunnett's test for multiple comparisons).
(**C,D**) Acute inhibition of LRRK2's kinase activity or of PI3-kinase reduced neuronal uptake of monomeric and aggregated tau. Neurons were preincubated with either 1µM LRRK2i (1) (GSK2578215A), 1µM LRRK2i (2) (MLi-2), 0.1 µM Wortmannin or vehicle control (0.1% DMSO). Histograms report tau uptake at final timepoint (dashed lines), which was significantly reduced by all treatments for both monomeric and aggregated tau. Minimum of 2 wells per treatment, and average of 9 fields of view per well. Error bars indicate SD. Significance was determined using one-way ANOVA (n = 3; $^{*}p < 0.05$, $^{**}p < 0.005$, and $^{***}p < 0.0001$, Dunnett's test for multiple comparisons).
(E) None of the treatments were acutely toxic to neurons, as reflected in extracellular LDH activity, in the presence of no treatment, vehicle (0.1%DMSO), 1µM LRRK2i (1) (GSK2578215A), 1µM LRRK2i (2) (MLi-2) or 0.1 µM Wortmannin (3 wells per treatment; 2 independent experiments). Error bars indicate SD. Significance was determined using one-way ANOVA (n = 3; $^{*}p < 0.05$, $^{**}p < 0.005$, and $^{***}p < 0.0001$, Dunnett's test for multiple comparisons).

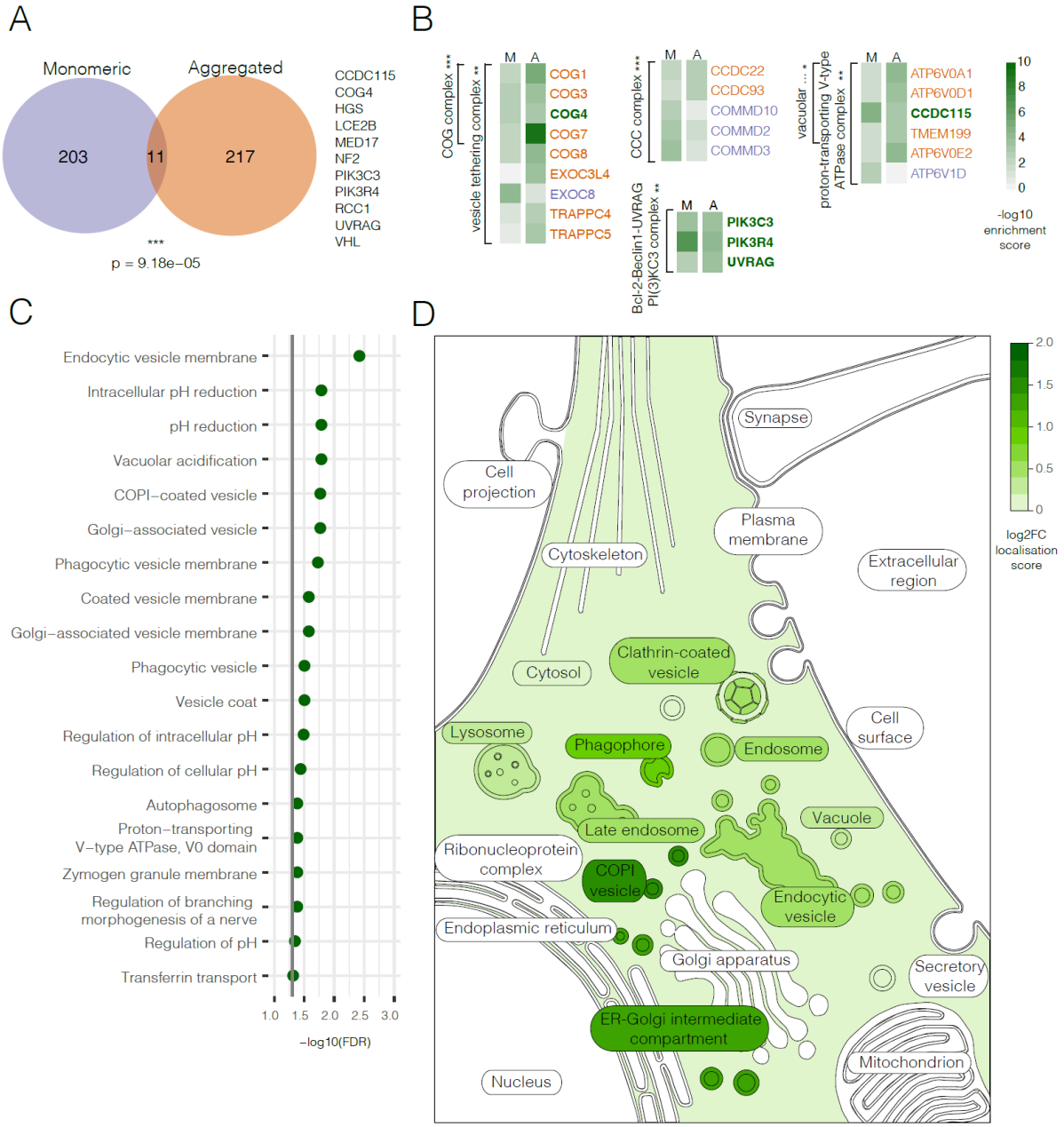

Figure 5: Monomeric and aggregated tau use similar mechanisms for neuronal entry

A. Genes identified as required for monomeric or aggregated tau uptake are significantly overlapping (hypergeometric test, p<0.001). The 11 genes identified in both screens are shown on the right side.

B. Subunits of protein complexes that are significantly enriched in the combined set of genes required for uptake of either form of tau. The colour indicates the strength of enrichment, and only subunits identified as required in either screen are shown (orange if identified in aggregated screen, purple if identified in monomeric screen, bold green if identified in both). M: monomeric screen; A: aggregated screen; p-value < 0.05 (*), <0.01 (**), < 0.001 (***).

C. Functional annotations enriched among 438 genes required for either monomeric or aggregated tau uptake(representative selection).

D. Genes required for either monomeric or aggregated tau uptake code for proteins with a significantly higher than random localisation score in particular cellular compartments in the COMPARTMENTS dataset (FDR < 0.05). Significantly enriched compartments are coloured based on the strength of enrichment (log2 fold-change) whereas non-significant compartments are left white.

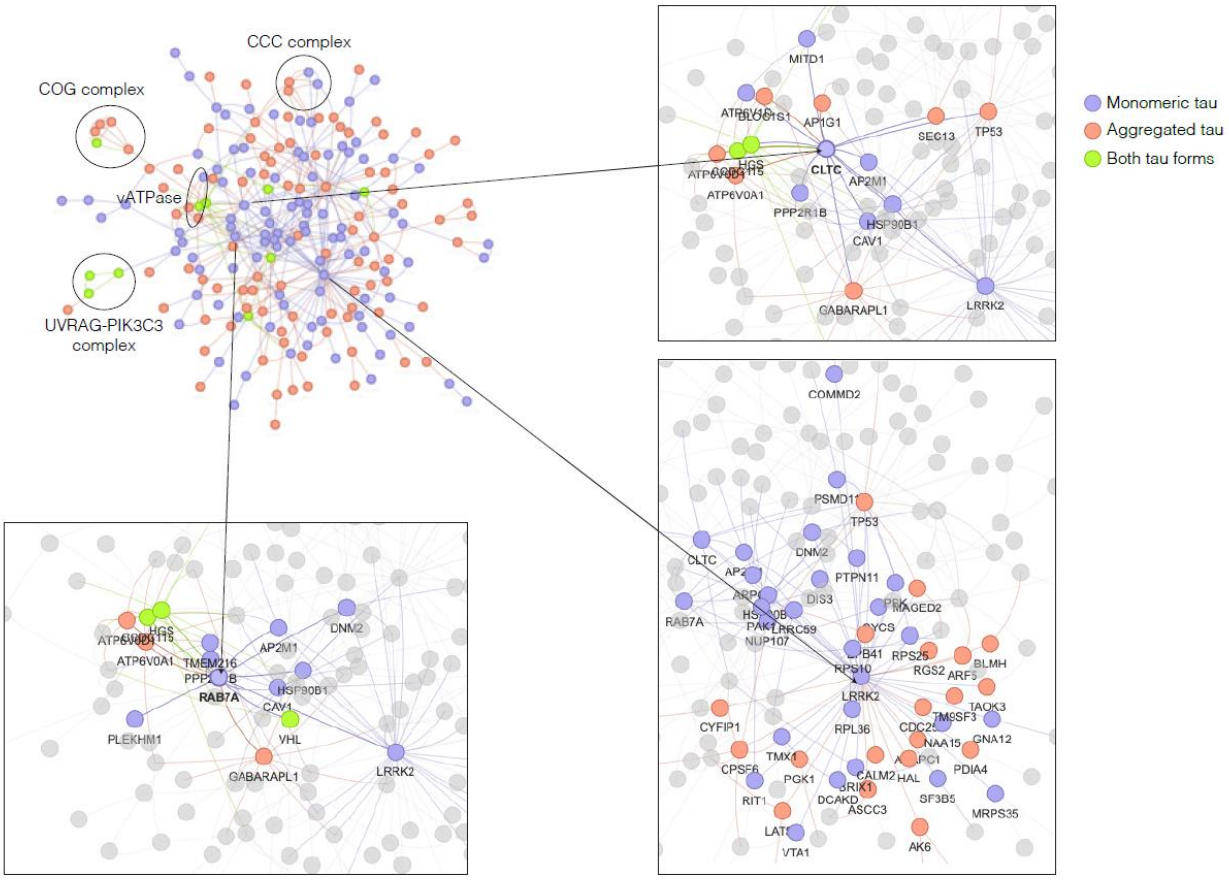

Figure 6: Cellular mechanisms for tau uptake and processing by human excitatory neurons

PSICQUIC-derived network of experimentally validated physical interactions between proteins encoded by genes identified in either screen. Nodes are colour-coded depending on whether the corresponding gene was identified as required for monomeric or aggregated tau uptake, or both. Some notable complexes are highlighted with circles. The direct interactors of LRRK2, CLTC, and RAB7A, among the most connected nodes, are shown in separate details surrounding the network. Interactions disconnected from the main network are not shown.

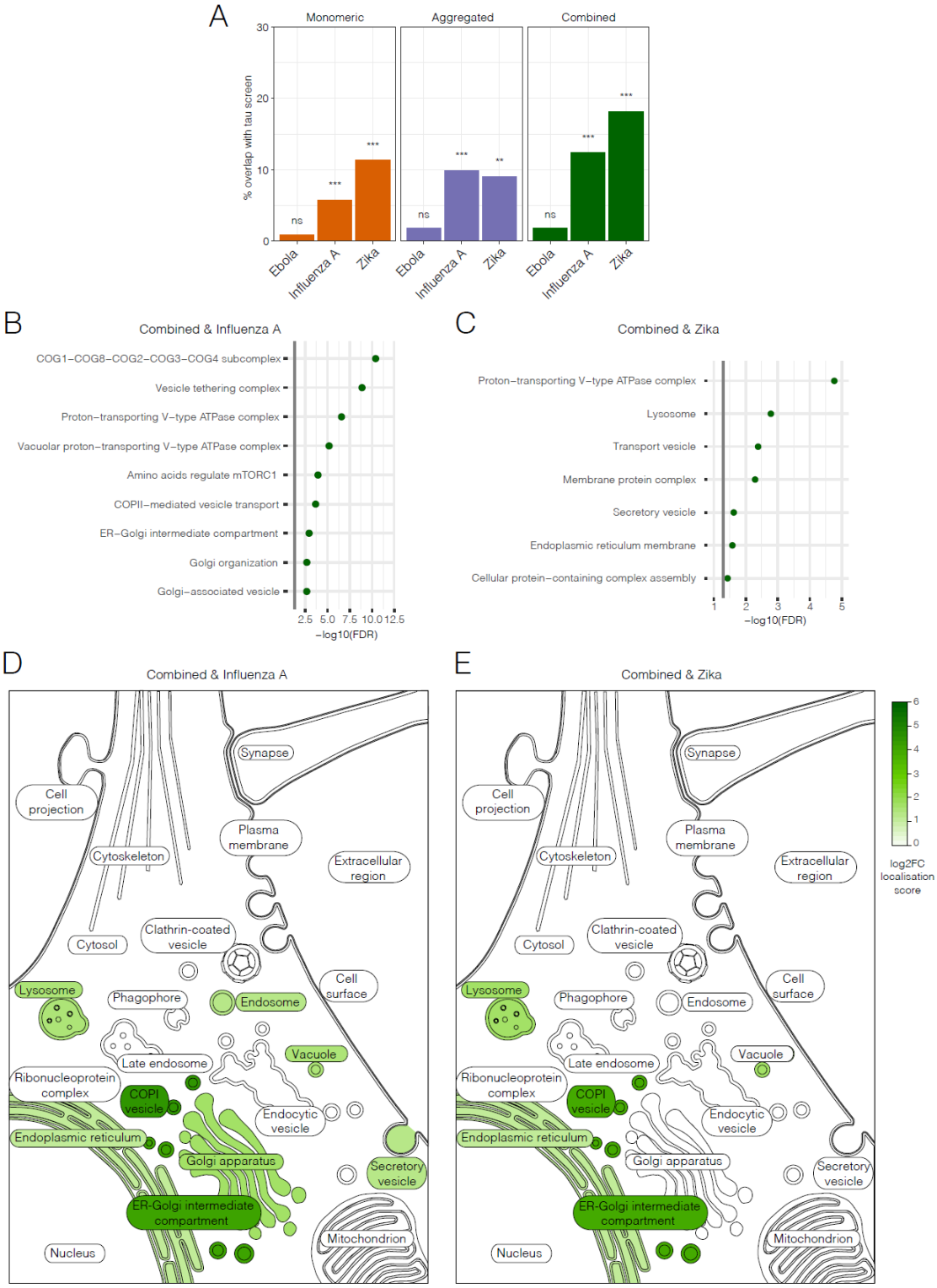

Figure 7: Neuronal uptake of extracellular tau shares functional similarities with receptor-mediated viral entry

A. The sets of genes required for aggregated tau uptake or monomeric tau uptake significantly overlap with the sets of genes required for cellular uptake of the Influenza A and

Zika viruses, but not the Ebola virus (hypergeometric test, p-value < 0.01 (**), < 0.001 (***); ns: not significant).

B-C. Functional annotations enriched among 15 genes required both for uptake of Influenza A virus and for either aggregated or monomeric tau uptake (B) or among 8 genes required both for uptake of Zika virus and for either aggregated or monomeric tau uptake (C) (representative selection).

D-E. Genes required for uptake of Influenza A virus and for either aggregated or monomeric tau uptake (D) and genes required for uptake of Zika virus and for either aggregated or monomeric tau uptake (E) code for proteins with a significantly higher than random localisation score in particular cellular compartments in the COMPARTMENTS dataset (FDR < 0.05). Significantly enriched compartments are coloured based on the strength of enrichment (log2 fold-change) whereas non-significant compartments are left white.

SUPPLEMENTARY FIGURE 1

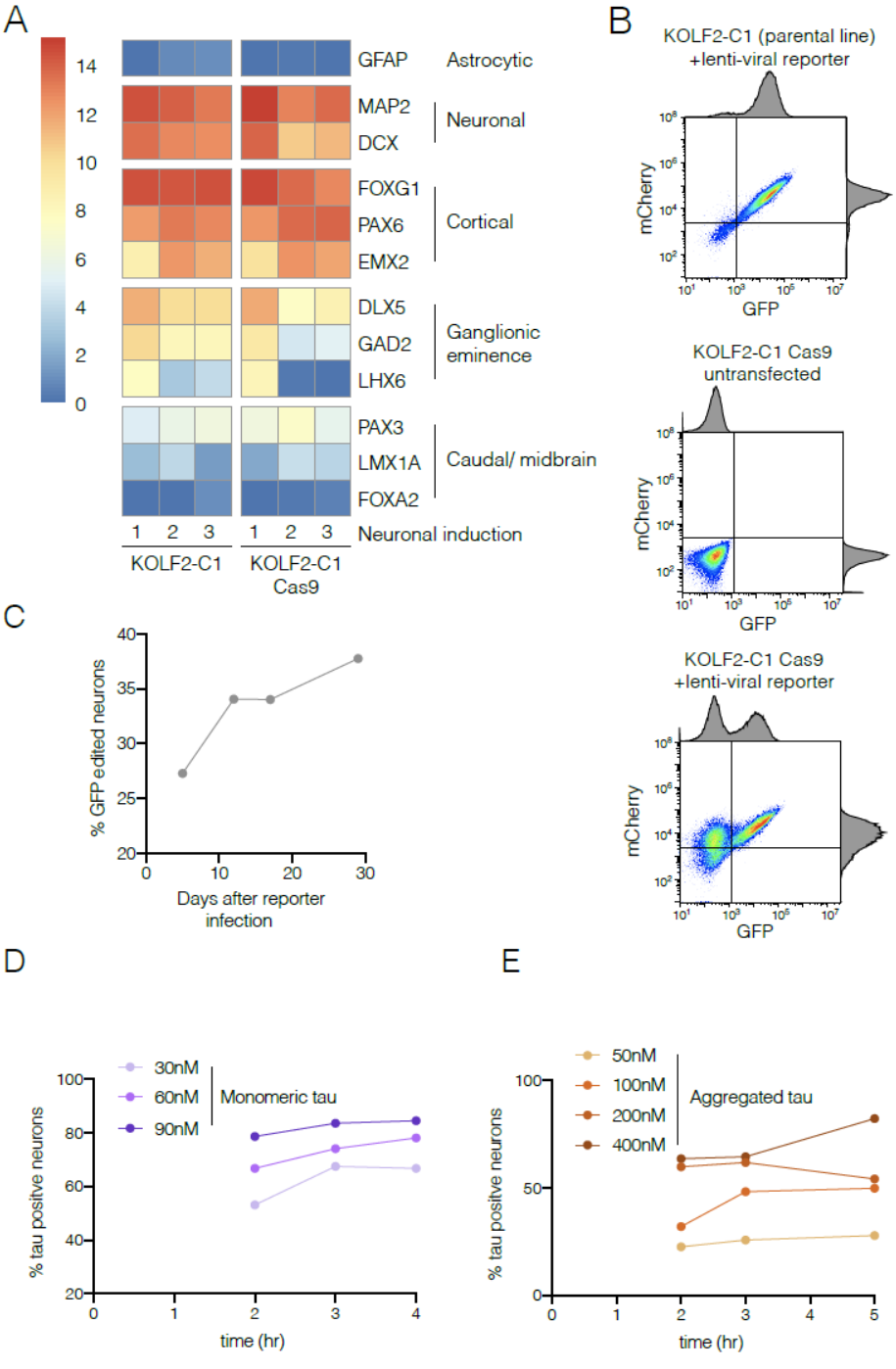

Supplementary Figure 1: Development and optimisation of CRISPR screen for tau uptake in human iPSC-derived excitatorty neurons

A. Gene expression analysis of iPSC-derived neuronal progenitor cells from KOLF2-C1 (parental line) and KOLF2-C1 Cas9 (constitutively expressing Cas9), 35 days after induction.

Selected genes whose expression is specific or enriched in particular regions and/or cell types are shown from a panel of 200 genes (see Experimental Procedures for details).

B. iPSC-derived neural progenitor cells and neurons retain Cas9 activity after differentiation. Scatterplot of FACS measuring Cas9 activity using lentiviral-expressed Cas9-activity reporter, expressing mCherry and GFP. Upper panel, KOLF2-C1 (parental control line) infected with lentiviral reporter but not expressing Cas9, middle panel KOLF-C1 Cas9 without lentiviral reporter and lower panel KOLF-C1 Cas9 with lentiviral reporter.

C. FACS analysis of percentage GFP gene-edited (knocked out) neurons against days after reporter infection, measured using reporter system described in B.

D, E. Optimising concentration of tau protein to achieve saturating levels of extracellular tau uptake during acute treatment, measured by flow cytometry. Graph reports percentage of tau-positive neurons against time after tau incubation initiation, with concentration of tau protein as indicated.